lubricants

MDPI

Article

Wear Properties of C-MoS_2-PTFE Composite Coating Prepared on 4032 Aluminum Alloy

Xuehui Chen [1,2], Yuxi Zhang [1,2], Congmin Li [3], Lei Huang [1,2], Yu Wang [1,2], Ting Gao [1,2], Zhenbin Zhang [1] and Wei Liu [1,2,*]

[1] School of Mechanical and Electrical Engineering, Anhui Jianzhu University, Hefei 230601, China
[2] Key Laboratory of Intelligent Manufacturing of Construction Machinery, Anhui Jianzhu University, Hefei 230601, China
[3] School of Mechanical Engineering, HeFei University of Technology, Hefei 230009, China
* Correspondence: liuwei@ahjzu.edu.cn; Tel.: +86-133-5560-2375

Abstract: A large number of joint friction pairs work during the work of scroll compressors, resulting in high energy consumption and short service life of scroll compressors. To improve the tribological performance of friction pairs of the scroll compressors, the C-MoS_2-PTFE (Polytetrafluoroethylene) lubrication coating is prepared through spraying technology on the surface of 4032 aluminum alloy, a common material for scroll compressors. The microstructure of the C-MoS_2-PTFE coating was analyzed by X-ray diffractometer (XRD) and scanning electron microscope (SEM), and the wear behavior of the coating under different loads was studied by reciprocating friction and wear testing machine and three-dimensional profiler. The surface of the grinding marks was analyzed by SEM and energy density spectrum (EDS). The performance was compared with the anodized film of 4032 aluminum alloy and the Ni-coated coating of 4032 aluminum alloy. The experimental results show that the C-MoS_2-PTFE coating has a dense structure, and the hardness is 35 $HV_{0.1}$. Under dry friction conditions, the C-MoS_2-PTFE coating has excellent wear reduction and wear resistance, and the coefficient of friction and wears rate under different loads are less than those of the anodized film of 4032 aluminum alloy and the Ni-plated coating. The wear mechanisms of C-MoS_2-PTFE coating are fatigue wear, adhesive wear, abrasive wear, and oxidation wear under different loads.

Keywords: 4032 aluminum alloy; C-MoS_2-PTFE coating; friction and wear; wear mechanism

Citation: Chen, X.; Zhang, Y.; Li, C.; Huang, L.; Wang, Y.; Gao, T.; Zhang, Z.; Liu, W. Wear Properties of C-MoS_2-PTFE Composite Coating Prepared on 4032 Aluminum Alloy. *Lubricants* **2022**, *10*, 181. https://doi.org/10.3390/lubricants10080181

Received: 19 July 2022
Accepted: 9 August 2022
Published: 10 August 2022

1. Introduction

4032 aluminum alloy has the advantages of low density, high strength, and easy processing and has been widely utilized in scroll compressors [1]. However, the fabricating and assembling process requires high accuracy due to the unique structural design, and the working mechanism of scroll compressors results in a large number of internal joint frictional pairs inescapable existence in scroll compressors, which cause enormous frictional work consumption losses during operation, making the input power increase and the operating efficiency lower [2]. However, the low hardness and poor wear resistance of 4032 aluminum alloy significantly limit its service life and reliability, so improving the frictional wear performance of 4032 aluminum alloy is the key to further improving the application of scroll compressors [3].

The surface modification methods of an aluminum alloy mainly include anodic oxidation, melt coating, and plating, and surface plating has the advantages of low cost and easy processing compared with other modification methods [4]. Polytetrafluoroethylene (PTFE) has the advantages of high-temperature resistance and low friction coefficient and has a wide range of applications in solid lubrication [5,6]. However, pure PTFE has poor wear resistance and load-bearing capacity, leading to reduced service life. Many scholars have modified PTFE and applied the modified PTFE coating to the surface of aluminum alloy. Liew K W [7] et al. studied the frictional wear performance of Ni-P-PTFE composite

coating on the surface of 7075 aluminum alloy at different rotational speeds and contact pressures. The experiments showed that Ni-P-PTFE composite coating could significantly reduce the wear performance of aluminum alloy, but the mechanical strength is low, and the wear resistance is limited. Sheng Q et al. [8] studied the friction and durability characteristics of PTFE films by vapor deposition on aluminum substrates with a thickness of 1 μm. The results showed that the protection of PTFE coatings against wear on aluminum alloy substrates gradually decreased with increasing surface roughness or sliding speed. Escobar J et al. [9] incorporated PTFE particles in the anodic oxide film on the surface of 1050 aluminum alloy. The results show that frictional wear experiments found that with the addition of PTFE particles, the real life of the anodic film was increased by 75 times, and the friction coefficient was reduced.

Filling wear-resistant materials in PTFE is the common approach, which not only improves the wear resistance of PTFE but also retains the advantages of PTFE material [10,11]. The wear-resistant materials like graphite, molybdenum disulfide and metal oxides can effectively enhance the formation of transfer films and reduce wear. Huang et al. [12] found that the hardness of PTFE composites increased significantly and varied flatly when the mass fraction of graphite was between 3% and 15%. In addition, they found that the wear rate of the composites decreased significantly when the mass fraction of graphite was 5%. Su et al. [13] investigated that MoS_2 could effectively reduce the friction coefficient of PTFE carbon fiber fabric composites. Lu et al. [14] found that Compared to a single AlCrN coating, the bond strength of the AlCrN-MoS_2/PTFE composite coating to the substrate is increased by about 15%, and the MoS_2/PTFE coating effectively reduces the friction coefficient of the AlCrN substrate. Chen Yi et al. [15] found that MoS_2 filling could effectively enhance the hardness of PTFE coatings, but the enhancement was not significant with the increased MoS_2 filling content. Wsa et al. [16] investigated the effect of MoS_2-filled PTFE lubricated coatings on the main properties of TiN coatings, and the experimental results indicated that the bonding force between TiN MoS_2/PTFE coatings and the matrix material increased the surface microhardness, the surface roughness, and the friction coefficient were significantly reduced. In addition, the MoS_2-filled PTFE lubricated coating could effectively improve the friction properties of conventional coatings.

In summary, filling PTFE with MoS_2 or graphite is a common way to improve its wear resistance, but there are few studies on it filled with MoS_2 and graphite to enhance the frictional wear performance. In this paper, the PTFE coating filled with graphite and MoS_2 was prepared on the surface of 4032 aluminum alloy by spraying technique, the common methods to reduce the wear of the frictional subsets of scroll compressors are embedded seals or surface treatment, and the main frictional conditions are dry friction [3,17]. Therefore, under dry friction, the tribological properties were compared with the traditional surface modification methods of aluminum alloy: surface anodizing and surface Ni coating, and the comparison showed that the C-MoS_2-PTFE coating has a greater advantage in wear reduction and abrasion resistance than the traditional surface modification methods [4]. And the tribological wear behavior of the coating was investigated, the wear morphology and composition of the coating were analyzed to reveal the tribological mechanism of C-MoS_2-PTFE coating.

2. Materials and Methods

2.1. Preparation of Specimens

The PTFE was modified by graphite and MoS_2, and the main composition of C-MoS_2-PTFE coating was shown in Table 1. As illustrated in Figure 1, 4032 aluminum alloy matrix material was cylindrical with a diameter of 28 mm and a thickness of 2 mm to simplify experiments. The coating surface was polished and cleaned before the test, and the coating surface was sandblasted to enhance the bonding between the coating and the matrix material. After sandblasting, a 3 μm thick C-MoS_2-PTFE coating is uniformly applied to the surface of 4032 aluminum alloy using a spraying process [18]. The specimens were placed in a muffle furnace at 380 °C for 15 min to cure the modified PTEF coating at a constant

temperature after spraying. The surface of the 4032 aluminum alloy was polished, and the Ni-coating specimens of the 4032 aluminum alloy through electroplated on the surface of the 4032 aluminum alloy. The surface of 4032 aluminum alloy is polished, and the surface anodized specimens of 4032 aluminum alloy were formed by putting 4032 aluminum alloy into the electrolyte solution for electrolytic treatment.

Table 1. Main components of C-MoS_2-PTFE coating.

Name	PTFE	C	MoS_2
Content	80–90%	5–10%	5–10%

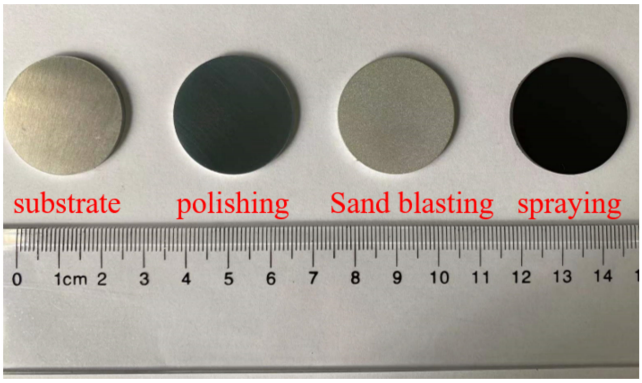

Figure 1. Specimen preparation process.

2.2. Tribological Test

The CFT-I Material surface performance comprehensive tester (Lanzhou Institute of Chemical Physics, Chinese Academy of Sciences, Lanzhou, China) carried out the test due to the advantage of the ball-plane contact method, such as a good contact state and easy analysis of damage forms. The friction pair was a 45# steel ball with a radius is 6 mm (hardness: 197 HV). The force loaded on the coating surface through 45 gauge steel balls is 5 N, 10 N, and 15 N, respectively. The experimental time was 30 min, and the frequency was 1 Hz. The experiment was repeated three times for each condition. The test was conducted at room temperature, and the computer automatically recorded the friction coefficient data. Figure 2 is a schematic diagram of the structure of the reciprocating friction and wear testing machine

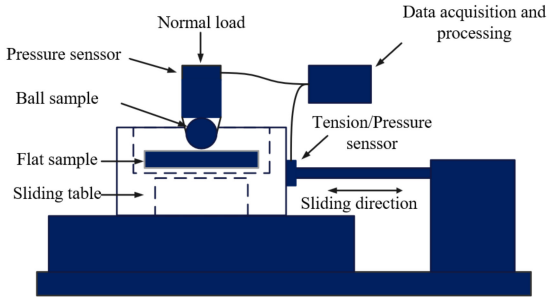

Figure 2. Structure diagram of reciprocating Friction and wear tester tribometer.

2.3. Plating Hardness Test

The Wilson Hardness 401MVD Microhardness Tester (BUEHLER, Chicago, IL, USA) was used to test the hardness of the coating. To avoid specimen deformation during the test, the test load is 100 gf and the load holding time is 10 s. Five tests were conducted at different selected locations on the coating surface to ensure the accuracy of the test data. The measurement points are spaced at 5 mm intervals, and the average value was taken to indicate the microhardness of the coating.

2.4. Analysis Method

The electronic analytical balance with the accuracy is 0.01 mg was used to weigh the mass of the specimens and the grinding balls before and after the wear test. Each data group was measured five times, and the average measured data was taken to reduce the testing error. The phase composition of the coating was analyzed using a DX-2700BH X-ray diffractometer (Cu target, 40 kV) (Dandong Haoyuan Instrument Co., LTD, Dandong, China). The Sigma-300 scanning electron microscope (SEM/EDS) (Carl Zeiss AG, Jena, Germany) was used to observe the microstructure of the coating and wear morphology and analyze the composition of specimens before and after the wear test. The Keyence VR-1000 3D profiler (KEYENCE, Osaka, Japan) was used to measure the 3D morphology of the specimens after the wear test.

3. Results and Discussion

3.1. Organizational Structure of C-MoS_2-PTFE Coating

Figure 3 shows the morphology of the C-MoS_2-PTFE coating surface, the cross-section morphology of the C-MoS_2-PTFE coating, the XRD pattern of the C-MoS_2-PTFE coating surface, and the EDS results of the C-MoS_2-PTFE coating surface. According to Figure 3a,b and e, the distribution of each element is uniform, and the surface of the C-MoS_2-PTFE coating is smooth, with good coverage and density. The coating was closely bonded to the matrix material, and cracks were not observed in the bonding area.

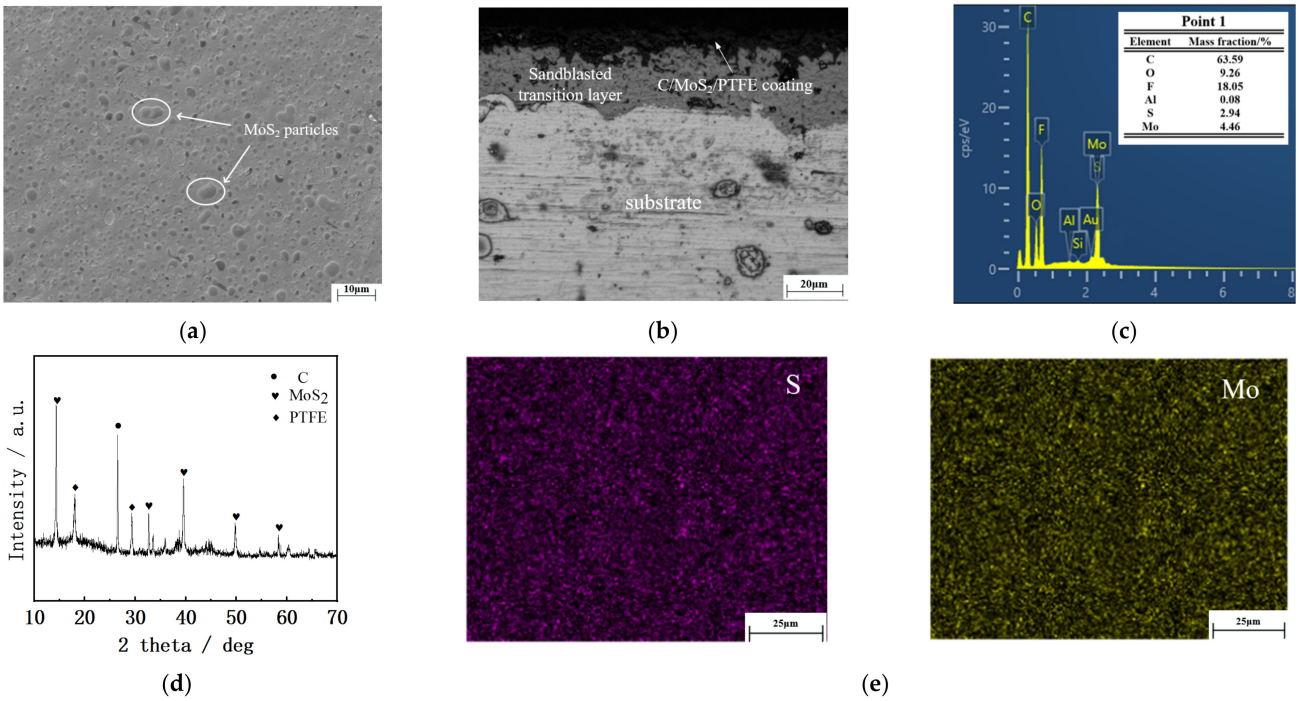

Figure 3. SEM morphology, surface XRD pattern, and EDS composition of C-MoS_2-PTFE coating surface and OM morphology of coating cross-section. (**a**) SME images of coated surfaces, (**b**) Optical microscopy of coating cross-section, (**c**) EDS analysis of coated surface, (**d**) XRD patterns of a Coated surface, (**e**) Element distribution diagram of coating material.

As illustrated in Figure 3c, the composition (atomic number fraction, %) of the elements on the surface of the C-MoS_2-PTFE coating was 63.59C, 9.26O, 18.05F, 2.96S, 4.46Mo. From Figure 3a,d, the modified coating is mainly composed of PTFE and diffusely distributed MoS_2 particles and C. These diffusely distributed MoS_2 particles can significantly improve the anti-wear performance of PTFE [19]. Graphite was added to the PTFE coating to reduce the friction coefficient and improve the wear resistance of the coating [20]. The average microhardness of C-MoS_2-PTFE coating was 35 $HV_{0.1}$.

3.2. Frictional Wear Performance of Modified PTFE Composite Coatings

The friction coefficient and wear depth change when the modified PTEF coating fails during the sliding wear. Therefore, observing the friction coefficient change and wear depth in the wear process can help judge the failure of the coating. The wear failure behavior of the modified coating can be directly revealed by observing and analyzing the wear marks on the coating surface after the wear test [21].

Figure 4a–c is the friction coefficients of C-MoS_2-PTFE coating, 4032 aluminum alloy anodic oxide film, and Ni-plated coating. Figure 4d is the friction coefficients of modified PTFE coating under different loads. According to Figure 4, the friction coefficient curves under different loads can be roughly divided into the rising, falling, and steady stages [22]. At the rising stage, as the reciprocal wear test continues, the C-MoS_2-PTFE coating/4032 aluminum alloy anodic oxide film/Ni-plated adhesive layer decomposed and peeled off as the reciprocal wear test starts. Direct contact occurs between the ball and C-MoS_2-PTFE coating/4032 aluminum alloy anodic oxide film/Ni-plated coating, increasing the friction coefficient continuously and reaching the maximum value. The coefficient of friction began to decline with the generation of grinding debris which can play a certain role in lubrication. The friction coefficient reaches a steady stage with the generation and discharge of debris in a relatively stable state. As illustrated in Figure 4a–c, the friction coefficient of C-MoS_2-PTFE coating is more steady than C-MoS_2-PTFE coating/4032 aluminum alloy anodic oxide film/Ni-plated coating under 5 N/10 N/15 N loads, and the average friction coefficient is smaller than that of the anodized film as well as the Ni-plated coating [23].

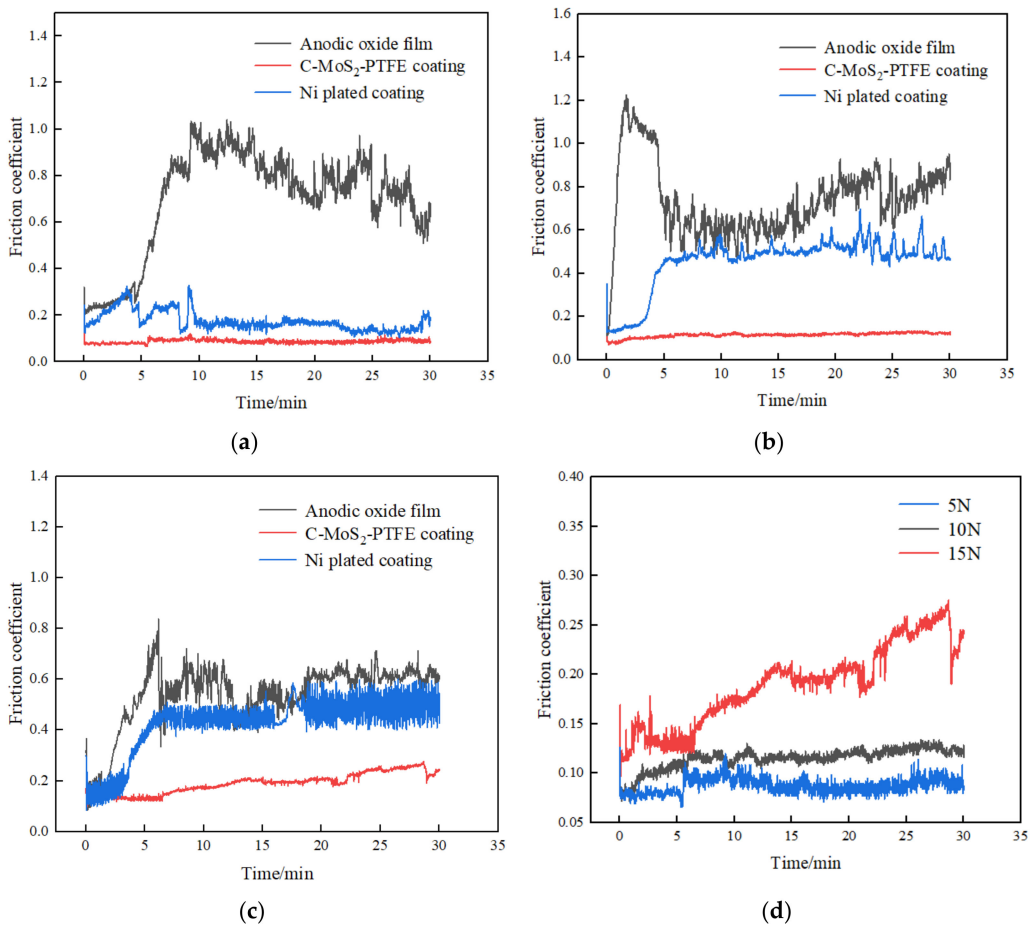

Figure 4. Friction coefficient under different loads. (**a**) 5 N, (**b**) 10 N, (**c**) 15 N, (**d**) Friction coefficient of C-MoS_2-PTFE coating under different loads.

Figure 4d shows that the average friction coefficients in the stable stage under different loads were 0.08–0.09 (5 N), 0.12–0.13 (10 N), and 0.2–0.21 (15 N), respectively. The average friction coefficient of C-MoS_2-PTFE coating gradually increased with the increasing load.

Equation (1) is used to calculate the wear rate of the coating [24].

$$Q = \frac{V_w}{NS} \quad (1)$$

where Q is the wear rate ($mm^3\ N^{-1}\ m^{-1}$), V_w is the wear volume (mm^3), N is the applied load (N), and S is the total sliding distance (m).

The wear rates of C-MoS_2-PTFE coating, 4032 aluminum alloy anodized film, and Ni-plated coating were calculated by Equation (1), and the results are shown in Figure 5. The wear rate of C-MoS_2-PTFE coating is much lower than that of 4032 aluminum alloy anodic oxide film and Ni-plated coating. The average wear rates of C-MoS_2-PTFE coatings under different loads are 0.4×10^{-5} $mm^3\ N^{-1}\ m^{-1}$, 0.6×10^{-5} $mm^3\ N^{-1}\ m^{-1}$, and 1.1×10^{-5} $mm^3\ N^{-1}\ m^{-1}$, respectively.

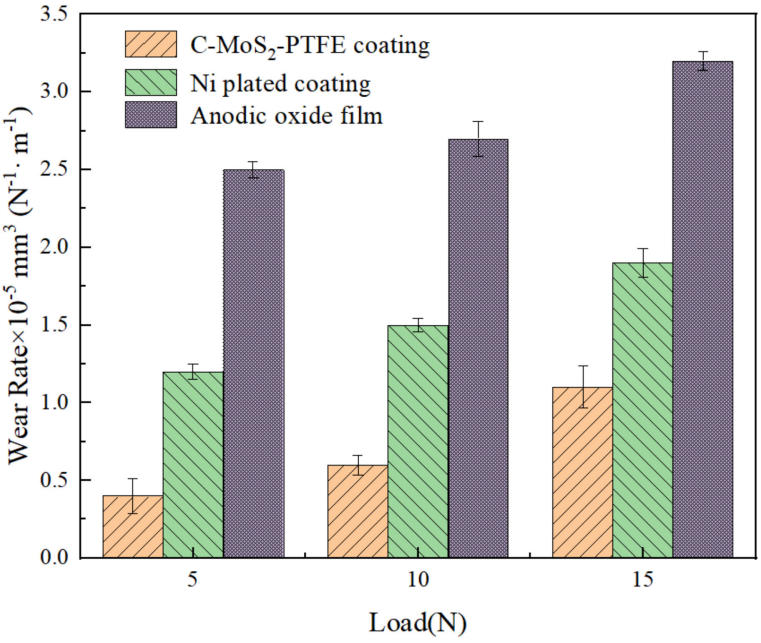

Figure 5. Wear rate under different loads.

The above results show that the friction coefficient and wear rate of C-MoS_2-PTFE coating is significantly lower than that of the 4032 aluminum alloy anodic oxide film and Ni-plated coating, which indicates that the modified PTFE coating can significantly improve the excellent friction and wear protection for 4032 aluminum alloy [25]. It also shows that adding graphite to the C-MoS_2-PTFE coating can significantly affect anti-wear lubrication.

3.3. Three-Dimensional Morphological Analysis of Wear

Figure 6 shows the three-dimensional morphologies of grinding marks on the surface of C-MoS_2-PTFE coating and 4032 aluminum alloy anodized film under different loads. The experimental results show that the cross-sectional profile is a "U" shape under loads of 5 N, 10 N, and 15 N. Besides, the area of the contact area and the area of the grinding marks increased with the load. The center of the grinding marks formed an elliptical crater, and the edge of the grinding mark had more debris accumulation. Due to the relative sliding of the ball and C-MoS_2-PTFE coating/4032 aluminum alloy anodized film, the micro-motion wear leads to the formation of larger pieces of debris on the surface of C-MoS_2-PTFE coating/4032 aluminum alloy anodized film. The debris is wear products of the plowed down 45# steel ball after grind and rubbing. Most of the debris discharged

from the friction surface with the wear proceeds, and the other debris participated in the frictional wear process and gradually formed a layer of wear products. Under different loads, the wear depth and area of the C-MoS_2-PTFE coating surface were much smaller than that of 4032 aluminum alloy anodized film, which indicates that the C-MoS_2-PTFE coating significantly improves its wear resistance compared to the base material [26].

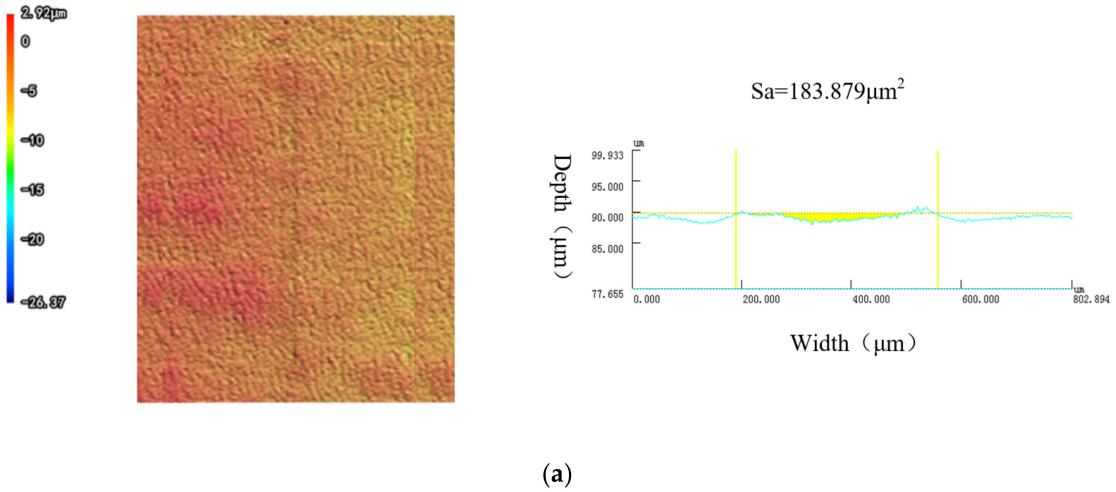

(**a**)

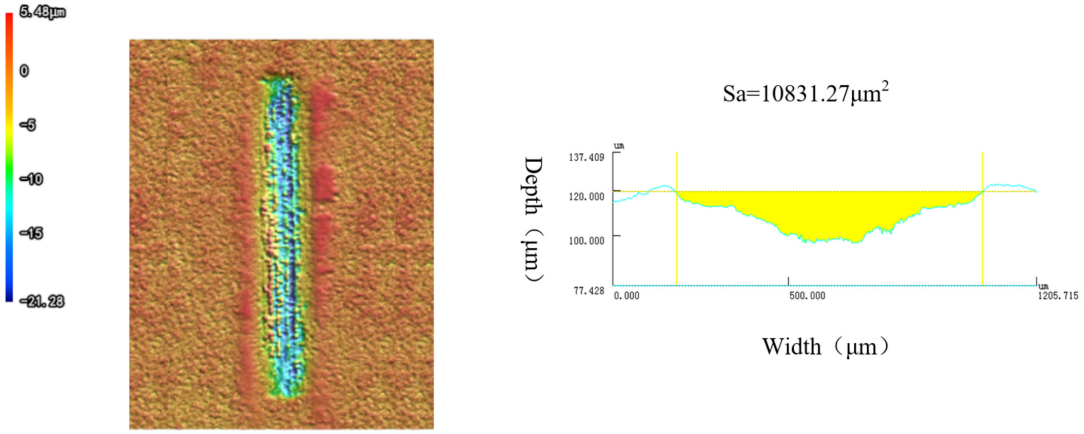

(**b**)

Figure 6. *Cont.*

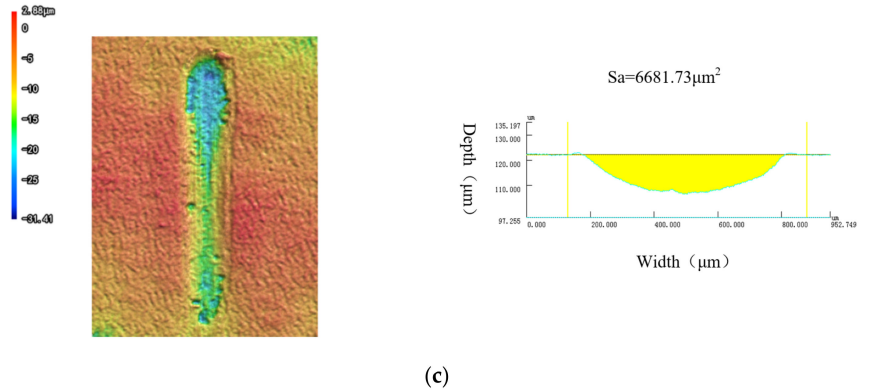

(**c**)

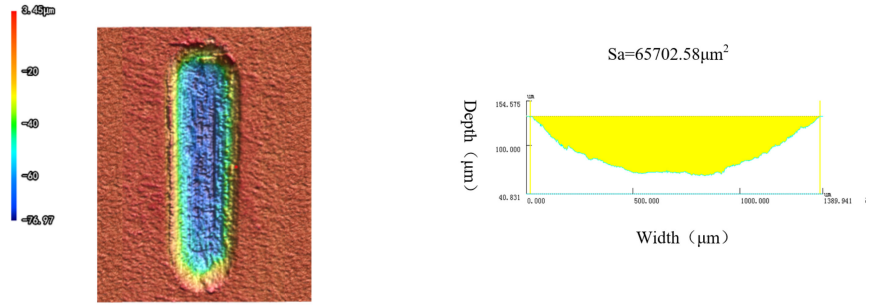

(**d**)

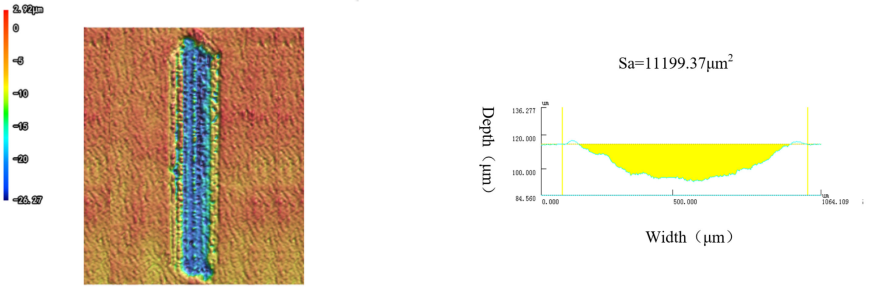

(**e**)

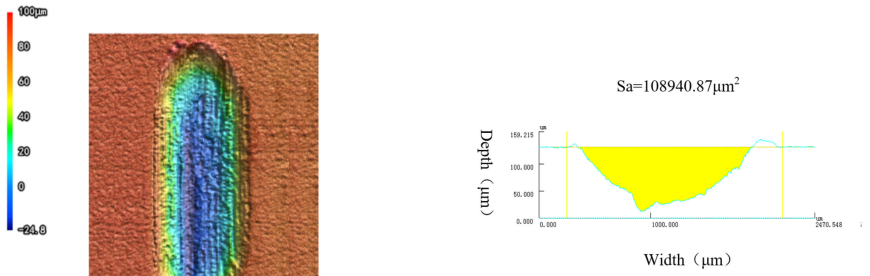

(**f**)

Figure 6. Three-dimensional wear morphology information of C-MoS_2-PTFE coating and anodized surface. (**a**)Three-dimensional morphology of wear scars of C-MoS_2-PTFE coating under 5 N load, (**b**) Three-dimensional wear morphology information of anodized surface under 5 N load, (**c**) Three-dimensional shape information of C-MoS_2-PTFE coating wear under 10 N load, (**d**) Three-dimensional wear morphology information of anodized surface under 10 N load, (**e**) Three-dimensional wear morphology of C-MoS_2-PTFE coating under 15 N load, (**f**) Three-dimensional morphology of anodic oxidation treatment table under 15 N load.

3.4. Microscopic Analysis of the Abrasion Mark Characteristics

Figure 7 shows the surface morphology of the wear surface after the wear experiment. Figure 8 shows the EDS analysis of the grinding mark of the specimen under different loads. The middle zone of the grinding mark is selected for analysis to ensure the accuracy of the experiment. From Figure 7, increasing the load widens the grinding marks obviously, because the increasing contact area makes debris discharge from grinding marks difficult. In the case of the 5 N load, the scaly tail crack and continuous and parallel furrows appeared in the abrasive marks, which indicates the milder wear process, and the wear mechanism is abrasive wear. It can be seen from Figure 8 that the O content in the wear area increases, indicating that oxidation wear occurs in the sliding process of the coating surface. When the load is 10 N, attachments and furrows appear on the grinding marks, and the width and depth of the grinding marks increase. During the sliding friction process, the frictional pair and the coating shed small debris due to the difference in hardness between the 45# steel ball and the C-MoS_2-PTFE coating and the frictional heat oxidized debris. The partial contact surface of the frictional ball oxidized under the combined action of contact stress and frictional heat, and the further stress cycle crushes the oxide iron. Therefore, the oxide debris of the 45# steel ball and C-MoS_2-PTFE coating accumulated between the ball and the coating, which formed the appearance of adhesive wear. The wear mechanism is fatigue wear gradually changed into adhesive wear and accompanied by oxidation wear. When the load is 15 N, the depth of the furrow becomes larger, and the modified coating starts spalling [27]. The elements (like Mg, Ca, Mn, and Ti) in EDS results are the elements of the 4032 aluminum alloy. According to EDS results, the C-MoS_2-PTFE coating failed after the wear experiment. The matrix material was exposed, and the wear resistance of the wear surface was reduced. The wear mechanism is the transformation from adhesive wear to fatigue wear.

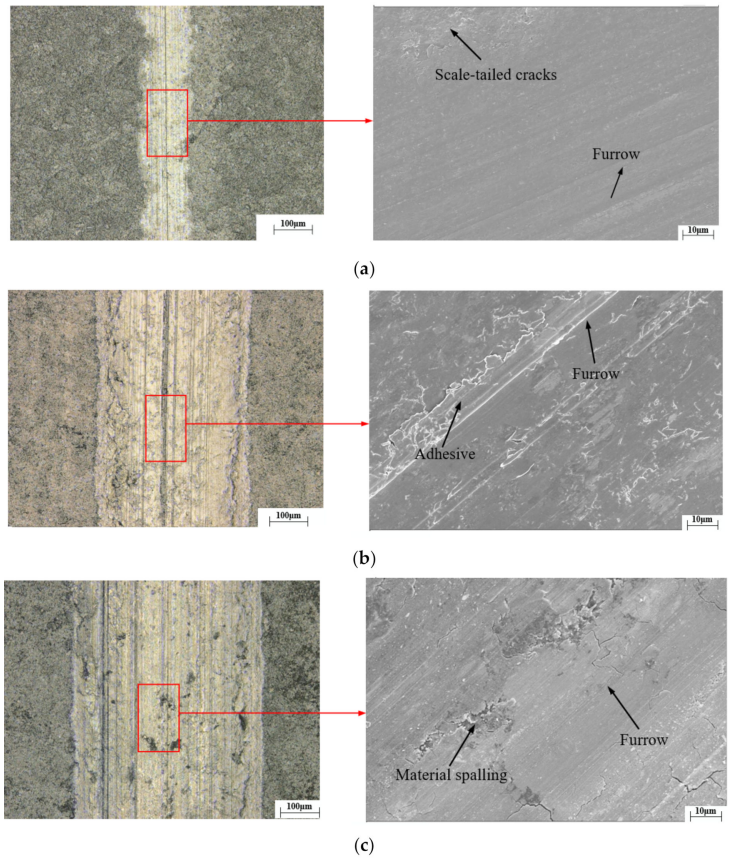

Figure 7. Worn surface morphology of C-MoS_2-PTFE coating under different loads. (**a**) 5 N, (**b**) 10 N, (**c**) 15 N.

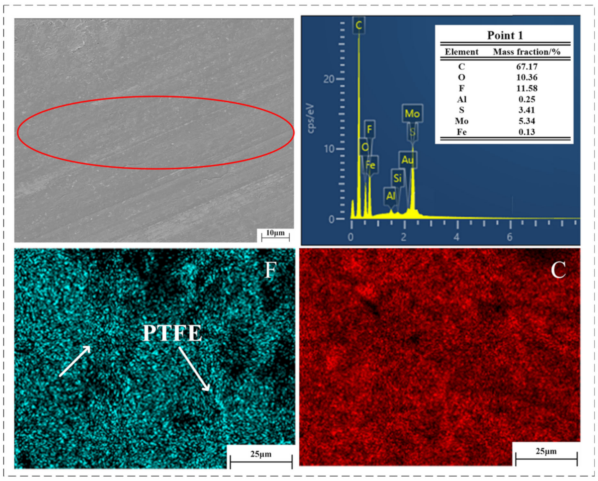

(**a**)

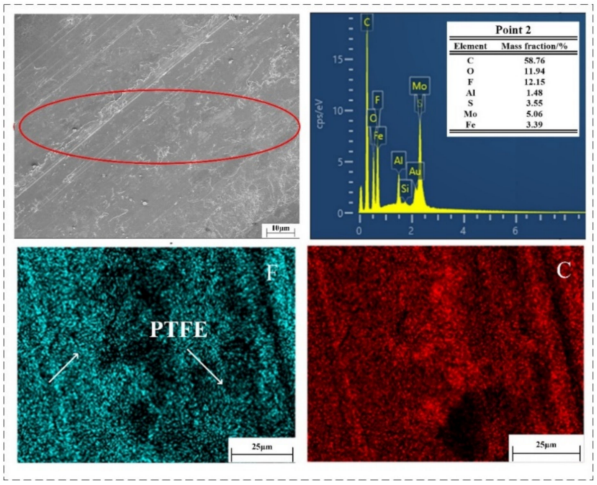

(**b**)

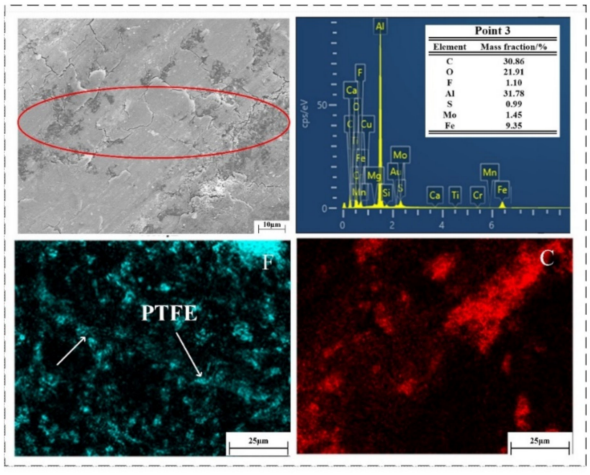

(**c**)

Figure 8. EDS surface scan image of surface wear of different loads modified C-MoS_2-PTFE coating. (**a**) 5 N, (**b**) 10 N, (**c**) 15 N.

In the process of the wear test, the debris is in a repetitive process of spalling and crushing due to the action of shear stress and normal stress between the 45# steel ball and C-MoS_2-PTFE coating/4032 aluminum alloy anodic oxide film/Ni-plated coating. The large size of the incipient debris accelerates the wear with the debris adheres to the frictional pair. As the increasing load, the process of increasing the coefficient of friction occurs earlier, and

the wear surface increases roughness and the friction coefficient. Meanwhile, the coating starts breaking and flaking, and the gradual failure of the coating increases the friction, leading to an increase in the coefficient of friction. Hence the larger the contact loads, the greater the coefficient of friction. The coefficient of friction coefficient under 15 N load specimens at 22 min suddenly and continuously increases because of the rupture failure of the coating and the contact friction of the 45# steel ball and matrix material coating [28].

The EDS results of the wear surface of C-MoS_2-PTFE coating under different loads and its elemental content are shown in Figure 8. Compared with the elemental content of the initial coating surface (Figure 3c), the C-MoS2-PTFE coating is worn with 45# steel under 5 N and 10 N load, but the wear did not cause serious spalling of the coating surface. Under 5 N load, the content of elements C, S, and Mo increased, and the content of element F decreased because the ability of MoS_2 to resist peeling was slightly greater than that of PTFE, and graphite had the self-lubricating effect. Under 10 N load, PTFE forms a transfer film, which plays a wear-resisting role, resulting in the content of element F increasing and the content of element C decreasing, while the of elements S and Mo change slightly. Under 15 N load, the coating peeled off and ruptured to expose the substrate, and the content of C, F, S, and Mo decreased significantly. The content of oxide on the wear surface of C-MoS_2-PTFE coating increases with the increasing load, which indicates that the more serious oxidative wear of the C-MoS_2-PTFE coating surface with the increasing load. The oxide layer spalls constantly owing to the easily cracked brittle oxide layer's friction load. Therefore, the coating and 45# steel ball wear surface are always in the dynamic process of oxidation → wear → re-oxidation → re-wear, and the oxidation aggravates the degree of wear between friction pairs [29]. The Fe element on the wear surface comes from the 45# steel ball frictional pair. The content of the Al element increases with increasing load due to the thickness of the C-MoS_2-PTFE coating constantly decreasing in the wear process, and cracks occur with the increase of load. According to the element distribution after the wear experiment in Figure 8a, the element distribution on the surface of the grinding marks is uniform at low loads. The low pressure and the temperature rise between the friction pair resulted in poor adhesion of the C-MoS_2-PTFE coating and the inability to form a complete transfer film. According to Figure 8b, the C element distributed on the grinding marks under 10 N load decreases, and the F element inside the grinding marks gradually extends in all directions to form a transfer film, and the surface C-MoS_2-PTFE coating is continuously protected by the transfer film formed during the wear process with an increasing number of cycles [30]. According to Figure 8c, the PTFE transfer film is continuously peeling off under high load with increasing wear, resulting in the exposure of the matrix material. At the same time, the peeling transfer film causes abrasive wear, which further increases the surface wear of the material. On the other hand, as the degree of wear increases, the oxidation on the surface of the grinding marks becomes progressively more severe.

4. Conclusions

The prepared C-MoS_2-PTFE coating has a dense organization, and the filled MoS_2 particles are evenly distributed in the PTFE material, which plays the role of dispersion reinforcement and improves the anti-wear effect of the coating. The filled graphite is also distributed uniform, which has a self-lubricating effect and plays a role in wear resistance, and PTFE can effectively form a transfer film during the wear process to reduce wear. Under dry friction conditions, the C-MOS_2-PTFE coating has a smaller friction coefficient and wear rate than 4032 aluminum alloy anodic oxidation film and 4032 aluminum alloy Ni coating with different loads, which shows a better wear reduction and lubrication effect. By comparing the three-dimensional morphologies of grinding marks under different loads compared with the anodic oxidation matrix material, the anti-wear performance of C-MoS_2-PTFE coating has also improved significantly, and the C-MoS_2-PTFE coating has a better anti-wear performance. The wear of the coating surface of the specimens increased with increasing load. For C-MoS_2-PTFE coating, When the load is 5 N, the wear process is

milder, and the wear mechanism is abrasive wear and oxidation wear; When the load is 10 N, C-MoS2-PTFE coating forms a transfer film, which forms a protective effect on the coating, and the wear process is more stable. The primary wear mechanisms are fatigue wear, slight adhesive wear, and oxidation wear. The coating ruptures when the load is 15 N, and the transfer film fails. The main wear mechanisms were adhesion wear, oxidation wear, and fatigue wear.

Author Contributions: X.C. and Y.Z. wrote the manuscript. C.L. and L.H. designed the study., Y.W., T.G., W.L. and Z.Z. developed the methodology. All authors have read and agreed to the published version of the manuscript.

Funding: This research was supported by the National Natural Science Foundation of China (Grant No. 51875152), the Anhui Province College Excellent Young Talents Fund Project (Grant No. gxyq2020034), Anhui Province Key Research and Development Program Project (2004a05020066, 202104a05020049). The Provincial Natural Science Key Research Project for Anhui Universities (KJ2020A0489).

Data Availability Statement: The data presented in this study are available on request from the corresponding author.

Conflicts of Interest: The authors declare no conflict of interest.

References

1. Wang, Y.F.; Zhao, S.D.; Guo, Y.; Yang, J.L. Effects of process parameters on semi-solid squeeze casting performance of aluminum alloy scrolls for scroll compressors. *China Foundry* **2020**, *17*, 27–36. [CrossRef]
2. Lin, Y.C.; Chen, H.H.; Chen, J.N.; Tang, Y.J.; Wang, B.C. Tribological Surface Modification for Thrust Bearing in Scroll Compressor. *J. Chin. Soc. Mech. Eng.* **2013**, *34*, 441–446.
3. He, Z.; Ji, L.; Xing, Z. Experimental Investigation on the DLC Film Coating Technology in Scroll Compressors of Automobile Air Conditioning. *Energies* **2020**, *13*, 5103. [CrossRef]
4. Bhat, K.U.; Panemangalore, D.B.; Kuruveri, S.B.; John, M.; Menezes, P.L. Surface Modification of 6xxx Series Aluminum Alloys. *Coatings* **2022**, *12*, 180. [CrossRef]
5. Unal, H.; Mimaroglu, A.; Kadioglu, U. Sliding friction and wear behaviour of polytetrafluoroethylene and its composites under dry conditions. *Mater. Des.* **2004**, *25*, 239–245. [CrossRef]
6. Burris, D.L.; Sawyer, W.G. Improved wear resistance in alumina-PTFE nanocomposites with irregular shaped nanoparticles. *Wear* **2006**, *260*, 915–918. [CrossRef]
7. Liew, K.W.; Chia, S.Y.; Kok, C.K.; Low, K.O. Evaluation on Tribological Design Coatings of Al_2O_3, Ni-P-PTFE and MoS_2 on Aluminium Alloy 7075 under Oil Lubrication. *Mater. Des.* **2013**, *48*, 77–84. [CrossRef]
8. Sheng, Q.; White, A.J.; Müftü, S. An Experimental Study of Friction and Durability of a Thin PTFE Film on Rough Aluminum Substrates. *Tribol. Trans.* **2015**, *59*, 632–640. [CrossRef]
9. Escobar, J.; Arurault, L.; Turq, V. Improvement of the tribological behavior of PTFE-anodic film composites prepared on 1050 aluminum substrate. *Appl. Surf. Sci.* **2012**, *258*, 8199–8208. [CrossRef]
10. Singh, H.; Sodhi, G.P.S.; Singh, M.; Chelliah, N.M.; Singh, H. Study: Wear and superhydrophobic behaviour of PTFE-ceria composite. *Surf. Eng.* **2018**, *35*, 550–556. [CrossRef]
11. Huang, R.; Ma, S.; Zhang, M.; Yang, J.; Wang, D.; Zhang, L.; Xu, J. Wear Evolution of the Glass Fiber-Reinforced PTFE under Dry Sliding and Elevated Temperature. *Mater. Lett.* **2019**, *12*, 1082. [CrossRef] [PubMed]
12. Huang, X.; Wan, F.; Chunxia, H.E. Performance Research on the Friction and Wear of the Polytetrafluoroethylene (PTFE) Modification Composite Filled with Nanometer and Nanometer Carbon Black. *Chem. Eng. Technol.* **2010**, *5*, 549–551. (In Chinese)
13. Su, F.H.; Zhang, Z.Z.; Wang, K.; Jiang, W.; Liu, W.M. Friction and Wear Properties of Carbon Fabric Composites Filled with PTFE and MoS_2. *JAPS* **2005**, *25*, 338–342.
14. Lu, Y.; Deng, J.; Song, W.; Li, X.; Zhang, L.; Sun, J. Tribological performance of AlCrN–MoS_2/PTFE hard-lubricant composite coatings. *Proc. Inst. Mech. Eng. Part J J. Eng. Tribol.* **2019**, *234*, 135065011987856. [CrossRef]
15. Chen, Y.; Yang, H.; Bian, D.; Zhao, Y. Study on the Tribological Properties of MoS_2 Composite Filled Modified PTFE Coating. *China Plast. Ind.* **2021**, *49*, 38–43. (In Chinese)
16. Song, W.; An, L.; Lu, Y.; Zhang, X.; Wang, S. Friction behavior of TiN–MoS_2/PTFE composite coatings in dry sliding against SiC. *Ceram. Int.* **2021**, *47*, 24003–24011. [CrossRef]
17. Wang, J.; Liu, T.; Sun, Y.; Mi, N. Research on Friction and Wear Characteristics of Tooth Tip Sealing Strip in Scroll Compressor. *Fluid Mach.* **2018**, *46*, 1–5. (In Chinese)
18. Ding, C.; Lin, H.; Sato, K.; Tsutai, Y.; Ohtaki, H.; Iguchi, M.; Wada, C.; Hashida, T. Preparation of Doped Ceria Electrolyte Films for SOFCs by Spray Coating Method. *J. Dispers. Sci. Technol.* **2009**, *30*, 241–245. [CrossRef]

19. Jiang, W.; Shen, L.; Qiu, M.; Xu, M.; Tian, Z. Microhardness, Wear, and Corrosion Resistance of Ni-SiC composite coating with Magnetic-Field-assisted Jet Electrodeposition. *Mater. Res. Express* **2018**, *5*, 096407. [CrossRef]
20. Sun, Y.; Wang, Y.; Li, Y.; Zhou, K.-C.; Zhang, L. Tribological behaviors of Aggraphite composites reinforced with spherical graphite. *Trans. Nonferrous Met. Soc. China* **2020**, *30*, 2177–2187. [CrossRef]
21. Shen, Y.; Lei, W.; Tang, W.; Ouyang, T.; Liang, L.; Tian, Z.Q.; Shen, P.K. Synergistic friction-reduction and wear-resistance mechanism of 3D graphene and SiO_2 nanoblend at harsh friction interface. *Wear* **2021**, *5*, 488–489. [CrossRef]
22. Li, H.; Jiao, L.; Xu, R.; Li, F.; Lu, S.; Qiao, Y.; Li, C.; Zhang, P. Surface Wear Behavior and Friction and Wear Mechanism Studies of A356/3wt.% Al 3 Zr Composites. *J. Mater. Eng. Perform.* **2021**, *30*, 3892–3902. [CrossRef]
23. Xie, X.; Zeng, Z.; Luo, J.; Xu, J. Friction and wear characteristics of linear contact sliding friction pairs under oil-air lubrication. *J. Braz. Soc. Mech. Sci. Eng.* **2021**, *43*, 356–357. [CrossRef]
24. Şenel, M.C.; Kanca, Y.; Gürbü, M. Reciprocating sliding wear properties of sintered Al-B_4C composites. *Int. J. Miner. Metall. Mater.* **2022**, *29*, 1261–1269. [CrossRef]
25. Tian, J.; Zhang, C.; Li, X.; Lai, S.; Xie, W.; Tian, W. Wear Behavior of Silicon-Cobalt Composite Coating Deposited on TiAl Alloy by Pack Cementation Process. *J. Mater. Eng. Perform.* **2022**, *31*, 4811–4819. [CrossRef]
26. He, T.; Song, G.; Shao, R.; Du, S.; Zhang, Y. Sliding Friction and Wear Properties of GCr15 Steel under Different Lubrication Conditions. *J. Mater. Eng. Perform.* **2022**. [CrossRef]
27. Wu, Z.; Zhou, F.; Wang, Q. Friction and Wear Properties of CrSiCN/SiC Tribopairs in Water Lubrication. *J. Mater. Eng. Perform.* **2018**, *27*, 2885–2898. [CrossRef]
28. Zhu, Y.; Qu, H.; Luo, M.; He, C.; Qu, J. Dry Friction and wear properties of several hard coating combinations. *Wear* **2020**, *10*, 456–457. [CrossRef]
29. Li, Z.Y.; Cai, Z.B.; Cui, Y.; Liu, J.H.; Zhu, M.H. effect of oxidation time on the impact wear of micro-arc oxidation coating on aluminum alloy. *Wear* **2019**, *426*, 285–295. [CrossRef]
30. Wu, H.; Zhu, L.-N.; Yue, W.; Fu, Z.-Q.; Kang, J.-J. Wear-resistant and hydrophobic characteristics of PTFE/CF composite coatings. *Prog. Org. Coat.* **2019**, *128*, 90–98. [CrossRef]